CSIRO PUBLISHING

International Journal of Wildland Fire **2014**, *23*, 1016–1026
http://dx.doi.org/10.1071/WF13160

High-resolution observations of combustion in heterogeneous surface fuels

E. Louise Loudermilk[A,C], *Gary L. Achtemeier*[A], *Joseph J. O'Brien*[A], *J. Kevin Hiers*[B] and *Benjamin S. Hornsby*[A]

[A]USDA Forest Service, Center for Forest Disturbance Science, 320 Green Street, Athens, GA, 30602, USA. Email: gachtemeier@fs.fed.us; jjobrien@fs.fed.us; bhornsby@fs.fed.us
[B]Eglin Air Force Base, Jackson Guard, Niceville, FL, 32578, USA. Email: john.hiers@eglin.af.mil
[C]Corresponding author. Email: elloudermilk@fs.fed.us

Abstract. In ecosystems with frequent surface fires, fire and fuel heterogeneity at relevant scales have been largely ignored. This could be because complete burns give an impression of homogeneity, or due to the difficulty in capturing fine-scale variation in fuel characteristics and fire behaviour. Fire movement between patches of fuel can have implications for modelling fire spread and understanding ecological effects. We collected high resolution (0.8×0.8-cm pixels) visual and thermal imaging data during fire passage over 4×4-m plots of mixed fuel beds consisting of pine litter and grass during two prescribed burns within the longleaf pine forests of Eglin Air Force Base, FL in February 2011. Fuel types were identified by passing multi-spectral digital images through a colour recognition algorithm in 'Rabbit Rules,' an experimental coupled fire-atmosphere fire spread model. Image fuel types were validated against field fuel types. Relationships between fuel characteristics and fire behaviour measurements at multiple resolutions (0.8×0.8 cm to 33×33 cm) were analysed using a regression tree approach. There were strong relationships between fire behaviour and fuels, especially at the 33×33-cm scale ($R^2 = 0.40$–0.69), where image-to-image overlap error was reduced and fuels were well characterised. Distinct signatures were found for individual and coupled fuel types for determining fire behaviour, illustrating the importance of understanding fire-fuel heterogeneity at fine-scales. Simulating fire spread at this fine-scale may be critical for understanding fire effects, such as understorey plant community assembly.

Additional keywords: fire heterogeneity, fuel type, image recognition, IR imagery, longleaf pine, regression tree.

Received 19 September 2013, accepted 28 March 2014, published online 11 September 2014

Introduction

Quantifying fire spread through heterogeneous fuel beds and modelling fire behaviour to predict fire effects has been elusive in fire science. This could be because complete burns give an impression of homogeneity in fire behaviour and fire effects, or due to the difficulty in capturing fine-scale variation in fuel characteristics and fire behaviour. How fire moves between patches of fuel can have important implications for understanding and predicting both fire spread and ecological effects. In frequently burned forests, connecting larger scale patterns of forest structure to small scale patterns in understorey plant diversity is critical to guiding silviculture and fire management (Mitchell *et al.* 2006; Thaxton and Platt 2006; Mitchell *et al.* 2009; Gagnon *et al.* 2012). Determining the mechanisms of fire-fuel synergisms that determine fire effects is the critical first step in making the links to those coarser scales. The principle of the ecology of fuels (Mitchell *et al.* 2009) applied to the longleaf pine (*Pinus palustris*) ecosystem highlights the important role of fine-scale variation in vegetative fuels that drive changes in fire behaviour. Intuitively, fine-scale variation of fire behaviour seems a likely determinant of plant community assembly in frequently burned longleaf woodlands because the high levels of diversity occur at scales too small (up to 50 species of vascular plants per square metre) for niche differentiation in the fairly uniform sandy soils that occur in the habitat (Kirkman *et al.* 2001).

Understanding fine-scale dynamics between fuel and fire provides a first step towards examining the role of fuel heterogeneity within stands at larger scales. As fire intensity is driven mainly by overstorey-derived fuels (i.e. pine litter, and more localised by pine cones) in these forests, understanding the relationship between the spatial patterns of fire-caused plant mortality (e.g. Wiggers *et al.* 2013) in the understorey and stand structure could provide a mechanistic link between management actions and patterns of understorey biodiversity and stand regeneration (O'Brien *et al.* 2008; Mitchell *et al.* 2009). Recent work has shown that fuels in longleaf pine woodlands are distributed in small scale (~0.5 m^2) patches that form discrete fuel 'cells' and have unique, yet non-linear combustion characteristics (Hiers *et al.* 2009; Loudermilk *et al.* 2012).

Understanding how fire moves between these patches of fuel has now been quantified, but the complexity of fuel arrangement reported to date challenges the capacity to model fire behaviour using current tools (Hiers *et al.* 2009).

The objective of this study was, firstly, to refine a fuel recognition technique that uses high-resolution imagery to classify fine-scale fuel types. These classifications will be used as inputs to Rabbit Rules (RR), an experimental coupled fire-atmosphere fire spread model (Achtemeier 2013). This entailed comparing classified and field recorded fuel types. Secondly, this study linked fine-scale classified fuel types with spatially explicit infrared measurements of fire behaviour to analyse, using a Classification and Regression Tree approach, how those fuel characteristics relate to fire behaviour at fine-scales. Fire behaviour in the context of this paper refers to the emitted radiation of a surface fire recorded with infrared thermography, and represented as pixel based fire radiative energy (J) and residence time.

Materials and methods

Study site

This study was conducted at Eglin Air Force Base during 2011. Eglin AFB, Niceville, FL, the former Choctawhatchee National Forest, is located on the panhandle of Florida, USA, and serves as an important reservoir for the longleaf pine ecosystem containing nearly 180 000 ha of longleaf pine and over half of the remaining old growth (Varner *et al.* 2000; Holliday 2001). The study site was within the Southern Pine Hills District of the Coastal Plain Physiographic Province with deep, well drained typic Quartzipsamments of the Lakeland series with mean depth to water table >200 cm (Overing *et al.* 1995). The climate of the area is subtropical, with warm, humid summers and mild winters. Mean annual temperatures in the area are 19.7°C, with a mean annual precipitation of 1580 mm, much of which falls from June to September (Overing *et al.* 1995). Elevations of the study sites were 52–85 m above sea level, and all sites had the minimal topography typical of sand hills (Myers 1990). Vegetation was dominated by a longleaf pine overstorey with a midstorey of various deciduous oaks, e.g. *Quercus laevis* Walter, *Q. margaretta* Ashe, *Q. incana* Bartram, *Q. germinata* Small. Typical fire return intervals are ~2–3 years.

Field fuel measurements

Within two separate prescribed burn units, two 4 × 4-m areas were used for this study to assess fine-scale (sub-metre) fuels and fire behaviour. Prior to each burn, 10 fuel clip plots (0.5 m^2) were randomly sampled within 10–20 m from around the perimeter of each 4 × 4-m plot. Burnable material was oven-dried at 70°C for 48 h and weighed to the nearest 0.01 g. The fuel bed within the first plot consisted mainly of loosely packed pine litter interspersed with tufts of grass consisting mainly of *Andropogon* and *Schizcharium* spp. A single oak bush (*Q. laevis*) and scattered forbs were also found within the plot. Fuel loads ranged between 0.303 and 0.617 kg m^{-2} with an average of 0.470 kg m^{-2}. The fuelbed within the second plot consisted of more firmly packed pine litter interspersed with tufts of *Andropogon* spp. and scattered pine cones. Fuel loads ranged between 0.416 and 1.009 kg m^{-2} with an average of 0.579 kg m^{-2}. Fuel type and height were also determined by point-intercept sampling on a 25-cm grid suspended over the 4 × 4-m plot. Typical fuelbed height was 0.10 m. A high resolution digital colour photo (using a 16 megapixel Canon Rebel Txi, Canon USA, Inc., Melville, NY, USA, with 28-mm lens) was taken from overhead at nadir of the fuel bed immediately before ignition. Fuel types were condensed into general fuel type categories to compare to the fuel types identified from the overhead images (described below in 'fuel recognition method'). For example, the perched pine litter category (pine litter suspended within the vegetation) was combined with the ground pine litter category, creating a simple 'pine litter' category.

Fire measurements

On 6 February 2011 (i.e. 'plot 1') and 14 February 2011 (i.e. 'plot 2'), a downward-pointing high resolution infrared thermography system captured fire spreading over the 4 × 4-m plots. The imaging system consisted of a 7 m-tall aluminium tripod with a FLIR (Forward Looking Infrared) SC660 (FLIR Systems Inc., Boston, MA, USA) thermal imaging system (Fig. A1) positioned directly above the 4 × 4-m plot. At this height and with the 45° optics used, the FLIR SC660 had a spatial resolution of ~0.8 × 0.8 cm per pixel (the SC660 microbolometer has an array of 640 × 480 pixels). Data were collected at 1 Hz. Further details on FLIR specifications are found elsewhere (e.g. Hiers *et al.* 2009, Loudermilk *et al.* 2012). Fire radiative power estimates were based on emitted infrared radiation and application of the Stefan–Boltzmann Law for a grey body emitter. Fire radiative energy (FRE) was the time integrated radiative power within pixels. The digital camera, used for fuelbed characterisation, was mounted next to the thermal imaging system.

Fire weather information for each burn was obtained from one of Eglin Air Force Bases' Improved Weather Dissemination System (IWDS, Eglin Air Force Base, Niceville, FL, USA) located on a bombing range less than 8 km from plot 1 and 6 km from plot 2. Weather data obtained from the IWDS for each burn was synchronised with fire incidence through the 4 × 4-m plots. IWDS data for plot 1 was: temperature, 12.1°C, relative humidity, 42%, average wind speed, 4.5 km h^{-1}. IWDS data for plot 2 was: temperature, 17.6°C, relative humidity, 43%, average wind speed, 12.4 km h^{-1}. Although this method does not show micro-site variation in weather parameters such as wind, it provides on-site weather parameters for each burn day.

Fuel recognition method

The digital photos (Fig. A2) were used for fuel recognition using RR. First, fuel types were visually identified in each image. For the first plot, six fuel types were identified, namely (1) grass (individual blades, clusters of blades and plants), (2) pine litter (fresh needles from the previous fall (autumn) deposited from scattered pine overstorey), (3) fermentation (F) layer (a mat of partially decayed grass, leaves and pine needles deposited two or more seasons before the burn), (4) oak leaves scattered from small bushes (one of which was located within the fuel bed), (5) live (non-dormant) vegetation and (6) a non-fuel type consisting of bare sand. For the second plot, four fuel types were

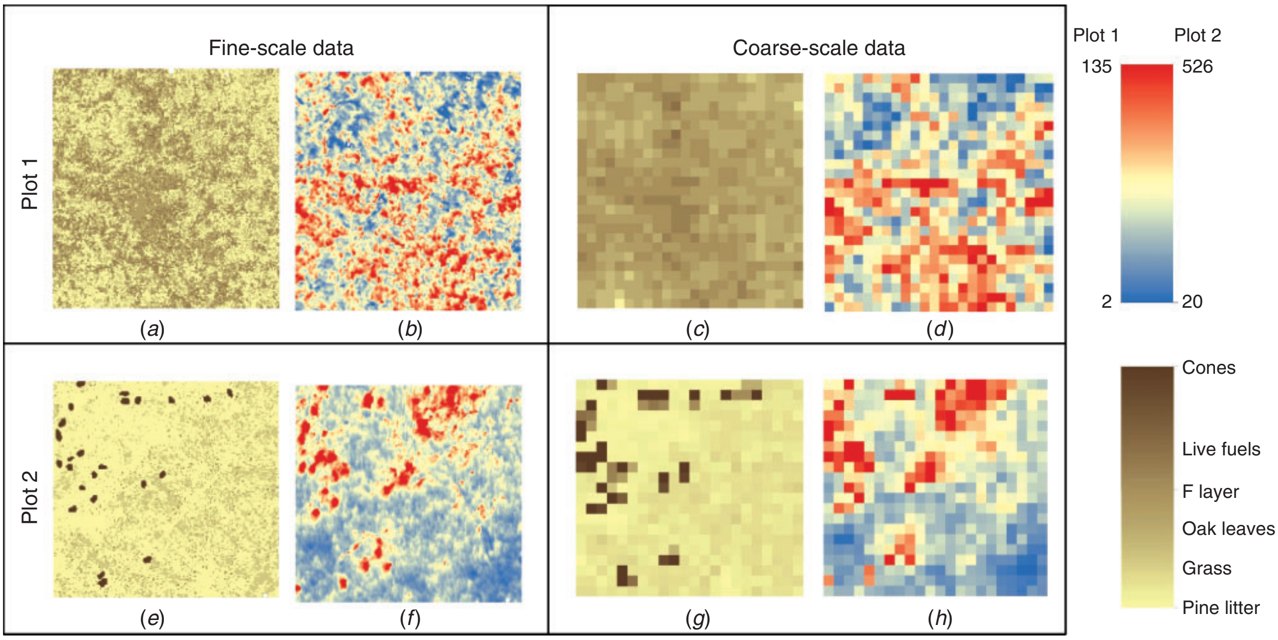

Fig. 1. Image classification of fuel types using the fuel recognition method coupled with known fuel characteristics (fuel proxy; *a*, *c*, *e*, *g*) as well as residence time (*b*, *d*, *f*, *h*) of fire collected from FLIR camera. Data is illustrated at the original (~0.8×0.8 cm) scale (*a*, *b*, *e*, *f*) and coarsened (~33×33 cm) scale (*c*, *d*, *g*, *h*). Plot 1: 1st row, Plot 2: 2nd row. Fuels legend corresponds to the fuel proxy values (see Fig. A3) and is an approximate scale dependent on fuels present in plot. Residence time is in seconds.

identified, namely (1) grass (individual blades, clusters of blades and whole plants), (2) pine litter (fresh needles from the previous fall deposited from the pine overstorey plus needle-fall from previous years), (3) pine cones and (4) live (non-dormant) vegetation. Live vegetation (fuels) was a small component, mainly consisting of some evergreen oaks (e.g. *Q.s virginiana*), vines (*Smilax* spp.) and saw palmetto (*Serenoa repens*).

Using a simple image editing program (Microsoft Paint), the colour characteristics of each fuel type were extracted. Then a list of colours including RGB components, fuel designation and fuel reference colour was passed through a colour identification scheme in RR and classified by designated fuel type colour (Fig. 1*a*, *d*). No field data on fuel types were used to develop or calibrate the fuel recognition classification technique.

CART analysis

We used a Classification and Regression Tree (CART) approach to analyse the relationships between the fire behaviour measurements and the image derived fuel types. CART has been successful in previous research where fine-scale fire-fuel relationships were non-linear (Loudermilk *et al.* 2012). CART is an alternative approach to multiple regression that can be used for simple or complex datasets (Breiman *et al.* 1984; De'ath and Fabricius 2000) and is useful in spatial ecology (Prasad *et al.* 2006; Grunwald *et al.* 2009). CART analysis uses a binary recursive partitioning approach, where the variation is iteratively split into more homogeneous (low-deviation) terminal nodes, which then determine their predictive ability (Grunwald *et al.* 2009). The CART analysis was processed using the 'rpart' library package in the R programming language (v3.0.1, R Core Team 2013). CART was run for each fire behaviour (response) variable, i.e. FRE (J) and residence time (above 300°C; s) within each plot. To create an independent fuel variable, the photo derived fuel types were categorised by their relative biomass and surface area. These categories were transformed by using an exponential function and known longleaf pine cone biomass (56.1 g; Fonda and Varner 2004) as an upper limit, to create a continuous fuel proxy variable (Fig. A3). These methods provided a simple, yet descriptive fuel variable that takes into account fuel type, biomass and surface area. This fuel proxy variable (called 'fuels' hereafter) and *x*- and *y*-coordinates (to account for spatial dependencies) were used as independent variables with each CART model. As the appropriate scale of measurement is unknown, but determined to be less than 1 m (Hiers *et al.* 2009; Mitchell *et al.* 2009; Loudermilk *et al.* 2012), we explored model fit at five scales: 0.8×0.8-cm, 4×4-cm, 8×8-cm, 16×16-cm and 33×33-cm resolution (e.g. Fig. 1). Four models (two fire behaviour response variables $\times$ two plots) were run at these five scales, resulting in 20 models in total. We assessed the relative contribution (explanatory power) of each independent variable within each model using the CART output variable importance rankings (Importance Value, IV). Within models, each variable is ranked from 1 to 100 using the 'rpart' package, where all the variable rankings total to 100.

Results

Field v. *image fuel types*

Fuel types classified by the fuel recognition approach using RR were comparable to the fuel types recorded in the field (Fig. 2). The two dominant fuel types (grasses and pine litter) as well as some less abundant, yet potentially important, fuel types

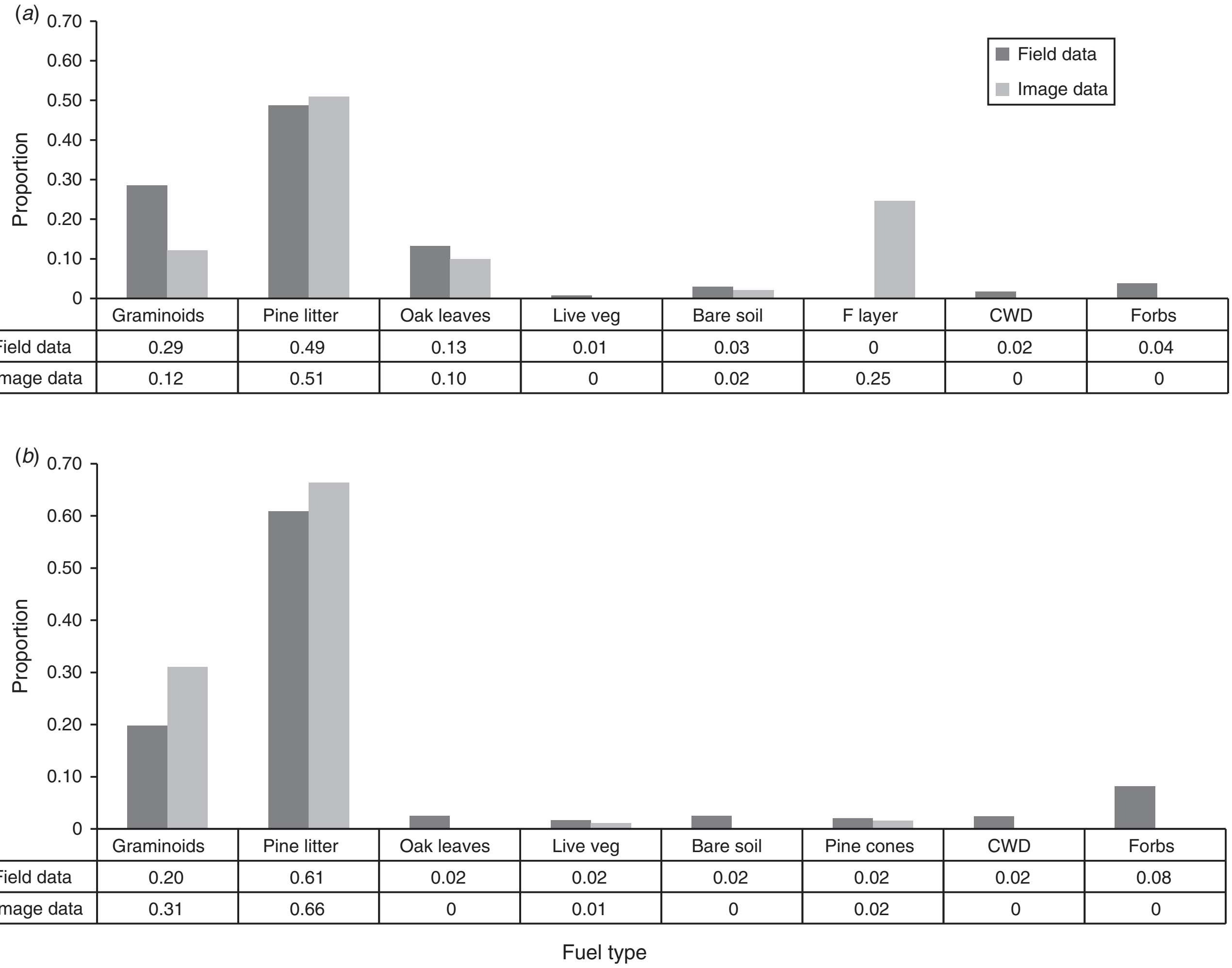

(a)

	Graminoids	Pine litter	Oak leaves	Live veg	Bare soil	F layer	CWD	Forbs
Field data	0.29	0.49	0.13	0.01	0.03	0	0.02	0.04
Image data	0.12	0.51	0.10	0	0.02	0.25	0	0

(b)

	Graminoids	Pine litter	Oak leaves	Live veg	Bare soil	Pine cones	CWD	Forbs
Field data	0.20	0.61	0.02	0.02	0.02	0.02	0.02	0.08
Image data	0.31	0.66	0	0.01	0	0.02	0	0

Fig. 2. Comparison of fuel types derived from high-resolution images (~0.8 × 0.8 cm) and field recorded data (25 × 25-cm point sampling) for plot 1 (*a*) and plot 2 (*b*), including a table of estimated proportions within each fuel type.

(e.g. pine cones, live vegetation) were well represented in both datasets. Discrepancies (e.g. grasses in plot 1) were likely due to resolution differences (image: 1 × 1 cm *v.* field data: 25 × 25 cm). Forbs and coarse woody debris were not categorised in the plot images, and were likely not identified because of their small proportion within the plot (<0.04), physical fuel overlap (obstruction), as well as colour similarities between fuels. The F layer was not an explicit fuel type category recorded in the field, but was recorded as oak or pine litter, or coarse woody debris that was partially decomposed.

Fuel types and fire behaviour

There were within and between plot differences in fuel type residence time and FRE (Figs 3, 4). For plot 1, mean residence time (mean (standard deviation, s.d.), s) (Fig. 3*a*) was highest for oak leaves (37.8 (12)) and F layer (37.6 (11)), followed by pine litter (34.9 (11)), live fuels (33.3 (9)) and grasses (31.3 (10)). Mean (s.d.) FRE (J) (Fig. 3*b*) was highest for live fuels (47.6 (20)), followed by oak leaves (44.9 (20)), F layer (41.7 (17)), pine litter (38.9 (17)) and grasses (38.0 (16)).

For plot 2, mean (s.d.) residence time (s; Fig. 4*a*) was by far highest for pine cones (187 (87)), followed similarly to plot 1, by pine litter (70.3 (31)), live fuels (65.8 (26)) and grasses (65 (30)). Mean (s.d.) FRE (J) (Fig. 4*b*) was highest for pine cones (310 (160)), followed by pine litter (94.2 (50)), live fuels (86.4 (41)) and grasses (86.1 (47)). The higher residence times and FRE estimates across fuel types in plot 2 were likely a product of the (23%) higher fuel loading and more fuel compaction, created by more overlaid leaf litter and grasses, that contributed to increased smouldering time. Pine cones are especially known to smoulder for extended periods (Fonda and Varner 2004). Residence times above 525°C were also explored (Table A1).

There were likely discrepancies between identification of fuel types, because of colour recognition issues (similar green or brown colours between fuels) as well as physical intergradation of various fuel types within the fuelbed. For instance, there was an obvious discrepancy for bare soil pixels in plot 1 (Fig. 3). Although bare soils had the lowest relative FRE, as expected, residence time was more intermediate. These bare soil pixels were small patches (<10 cm^2), and not likely large enough to

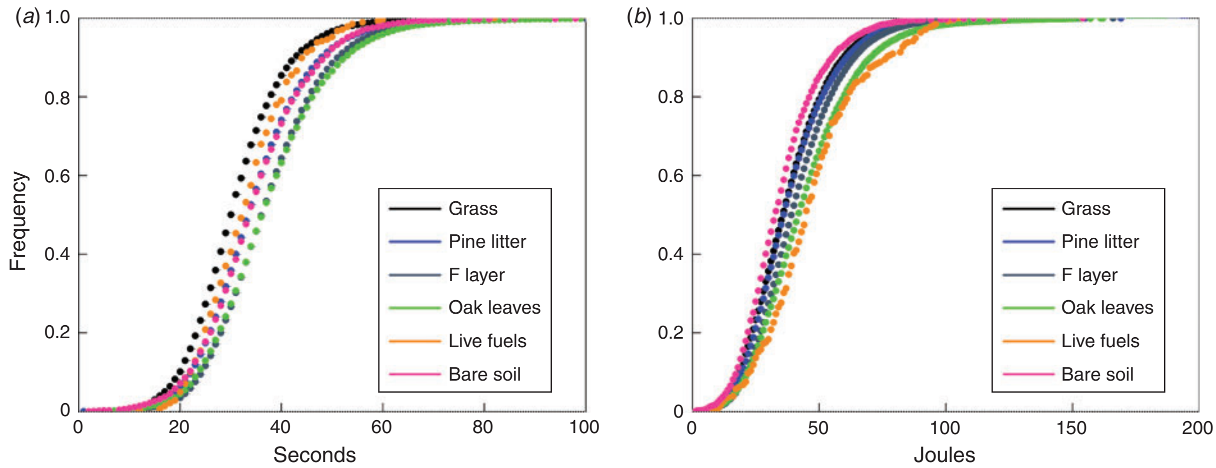

Fig. 3. Cumulative distribution of residence time (*a*) and FRE (*b*) from fire across image-derived fuel types for plot 1. Note the difference in scale of *a* and *b* between Figs 3 and 4.

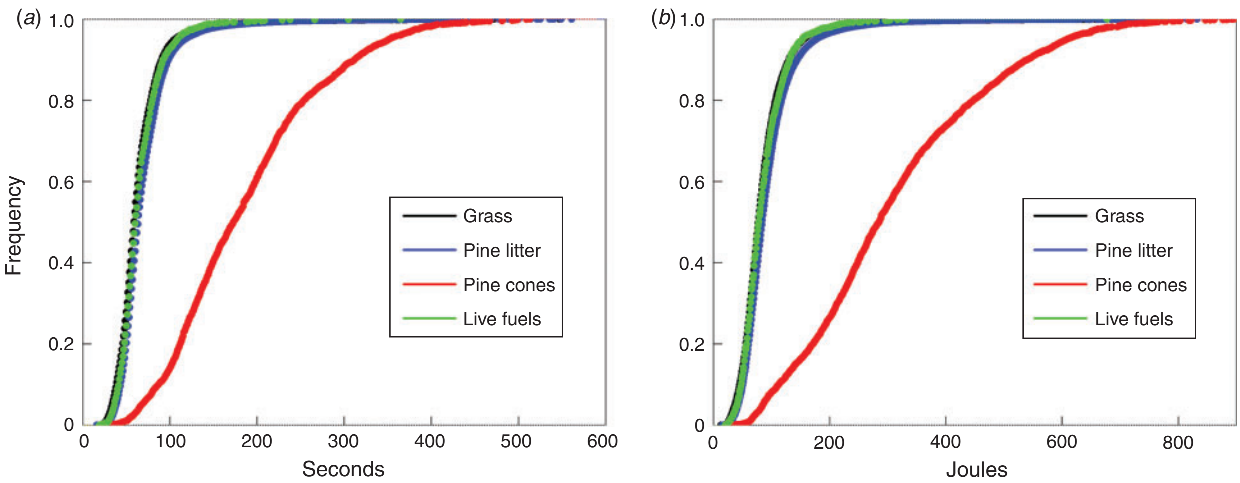

Fig. 4. Cumulative distribution of residence time (*a*) and FRE (*b*) from fire across image derived fuel types for plot 2. Note the difference in scale of *a* and *b* between Figs 3 and 4.

create a fire break that may disrupt fire spread across pixels. If the bare soil patches were large enough, there would be no FRE nor residence time estimates as fire would move around the patch. Furthermore, differences between pine litter, live fuels and grasses were less distinct in plot 2 than plot 1 (Fig. 3 *v*. Fig. 4). This was possible because of coupled effects from more physical overlap and higher loadings of fuels within plot 2. In addition, other woody fuels (including more pine cones) may have been missed (see Fig. 1).

CART results

Model strength varied from 0.08 to 0.69 R^2 among all models and was dependent on fuels within each plot as well as the scale of the model. Coarsening the resolution improved model strength (from $R^2 = 0.08$–0.40 to $R^2 = 0.40$–0.69), reduced RSE and improved variable predictive significance (IV) of the fuels within each model (Table 1). Plot 2 had stronger models ($R^2 = 0.34$–0.69) than plot 1 ($R^2 = 0.08$–0.40), and improved similarly across scales ($R^2 = 0.40$–0.69 at 33 × 33 cm). For plot 1, residence time and FRE models had similar performance, but fuels contributed more to the residence time models (IV = 15–48) than for FRE models (IV = 0–38). For plot 2, the FRE and residence time models also resulted in similar performance ($R^2 = 0.34$–0.69), although fuels contributed more to FRE models (IV = 54–65) than for residence time models (IV = 52–54). We explored CART models at coarser scales, up to 1 × 1 m. Model fit remained similar or slightly improved up to the 1 × 1-m scale, but at the cost of reducing the significance of fine fuels (e.g. grasses, pine litter) in the model and reducing fuel and fire heterogeneity across the plot.

For both plots, fuel types were best represented in the coarsest-scale models (see IVs, Table 1). Plot 1 illustrated, however, the greatest improvement of fuel representation through scaling, where error was reduced and fuel type representation was strong. For instance, pine litter was distinct from grasses. Also, pine litter combined with grasses was distinct

Table 1. CART model results, using fuels and *x*- and *y*-coordinates as predictor variables, across all scales of data
RSE, root square error; FRE, fire radiative energy

Plot	Model	Number of terminal nodes	Variable importance	Scale (resolution)	R^2	RSE
1	FRE (J)	2	*y* (100)	0.8 × 0.8 cm	0.10	16.45
	Fire Residence Time (s)	3	*y* (85), fuels (15)	0.8 × 0.8 cm	0.08	10.54
2	FRE (J)	10	fuels (54), *y* (33), x(14)	0.8 × 0.8 cm	0.40	46.25
	Fire Residence Time (s)	6	fuels (52), *y* (38), *x* (10)	0.8 × 0.8 cm	0.34	29.10
1	FRE (J)	6	*y* (79), *x* (14), fuels (8)	4 × 4 cm	0.15	15.52
	Fire Residence Time (s)	3	*y* (76), fuels (23), *x* (1)	4 × 4 cm	0.10	10.16
2	FRE (J)	9	fuels (56), *y* (33), *x* (10)	4 × 4 cm	0.45	44.68
	Fire Residence Time (s)	15	fuels (44), *y* (36), *x* (21)	4 × 4 cm	0.47	25.65
1	FRE (J)	6	*y* (76), *x* (13), fuels (11)	8 × 8 cm	0.18	14.00
	Fire Residence Time (s)	4	*y* (61), fuels (35), x(4)	8 × 8 cm	0.14	9.16
2	FRE (J)	10	fuels (60), *y* (30), *x* (9)	8 × 8 cm	0.48	40.69
	Fire Residence Time (s)	15	fuels (48), *y* (31), *x* (21)	8 × 8 cm	0.52	23.24
1	FRE (J)	10	*y* (64), fuels (21), *x* (15)	16 × 16 cm	0.28	11.22
	Fire Residence Time (s)	5	fuels (54), *y* (39), *x* (8)	16 × 16 cm	0.21	7.66
2	FRE (J)	10	fuels(65), *y* (27), x(9),	16 × 16 cm	0.57	33.18
	Fire Residence Time (s)	15	fuels (57), *y* (29), *x* (14)	16 × 16 cm	0.57	19.74
1	FRE (J)	6	*y*(62), fuels (38)	32 × 32 cm	0.40	8.18
	Fire Residence Time (s)	11	fuels (48), *y* (46), *x* (6)	32 × 32 cm	0.40	5.44
2	FRE (J)	13	fuels (65), *y* (27), *x* (9)	32 × 32 cm	0.69	23.78
	Fire Residence Time (s)	11	fuels (54), *y* (33), *x* (13)	32 × 32 cm	0.69	14.27

from oak leaves combined with live fuels (Fig. A4). For plot 2, fuels, driven predominantly by the presence of pine cones, were the main predictor. Using the fuel proxy approach allowed this less abundant fuel type to be represented across scales (i.e. no diminishing influence of pine cones as the scale coarsened; Fig. 1). In the coarsest model, and besides the significant influence from the pine cones, there was a distinction between pine litter and grasses (Fig. A5).

Discussion

From this study, we determined that the fuel colour recognition method for categorising fuel types from high-resolution imagery was successful at categorising fuel types and should be applicable for use in fine-scale fire behaviour modelling. This is the first known fuel recognition method for mapping fine-scale fuel types within a surface fuelbed, although fuel mapping has been done extensively across landscapes using other remote sensing techniques (e.g. Keane *et al.* 2001; Arroyo *et al.* 2008; Mutlu *et al.* 2008). Furthermore, fuel types were comparable to field data (Fig. 2), capturing both dominant (e.g. pine litter) and less abundant, yet important fuel types (i.e. pine cones). These image-derived fuel types demonstrated combustion variability between fine fuels (Figs 3, 4). For instance, within plot 1, where fuels were loosely packed and lighter compared to plot 2, residence times of combustion varied among grasses, pine litter and the F layer. Grasses and pine litter output similar FRE, although grasses burned for shorter durations than did pine litter and the F layer.

The CART analysis determined that image-derived fuel types coupled with other fuel properties correlated well to fine-scale fire behaviour. Model strength (up to 0.69 R^2) and fuel significance (IV) within each model was substantial (Table 1), especially considering the simple representation of fuels (Fig. 2). The CART approach showed how variation among various fine-fuels affected fire behaviour. Within plot 1, pine litter was distinct from grasses in determining fire behaviour, whereas pine litter combined with grasses was distinct from oak leaves and live fuels. Within plot 2, pine cones – a fuel type comprising <1% of the fuel types – was by far the most influential fuel type, followed by pine litter and live vegetation.

The scale of fuel estimation relative to fire behaviour was particularly important in the CART models. This suggests that fuel type (e.g. cones, litter, grass), their spatial combustion properties, and heterogeneity drive fire behaviour patterns. A scale of 33 × 33 cm was ideal for relating fuels and fire behaviour in our study. Identifying individual fuel types by pixel (e.g. original fine-scale data, <1 cm^2) was, however, important for quantifying fuelbed heterogeneity and creating the coarser scale models (up to 33 × 33 cm). Multiple fuels within a small area created a unique fuel environment, that when aggregated, corresponded well to observed differences in fire behaviour. Scaling the datasets also reduced potential error in classification (e.g. shadowing, misclassification, overlapping fuels) as well as overlay error between imagery datasets (fuel image *v.* FLIR images). This was likely inevitable because of micro-scale weather, combustion patterns (e.g. wind eddies) and small camera movements.

Although other fuel and fine-scale weather attributes (e.g. fuel depth, fuel moisture, wind, ambient temperature) were not included in the CART models, and can be important for modelling surface fires (e.g. Morvan and Dupuy 2001; Berjak and Hearne 2002), their inclusion was beyond the scope of this study and were most likely a component of the unexplained variation within each model (see Loudermilk *et al.* 2012). Here, we focused on determining if and how much of a connection exists from photo-derived fuel types (and their characteristics) and actual fire behaviour measurements at this scale, that would provide a foundation for running the RR fire behaviour model.

The fuel recognition method in RR for identifying fine-scale fuel types had its limitations. For instance, fuel types may have been misrepresented, or not represented at all, because of colour similarities between fuel types as well as physical overlap and obstruction. This was especially true for some less abundant fuel types, e.g. forbs and coarse woody debris (Fig. 2). These discrepancies increased the spread of distributions of fire behaviour measurements (e.g. Fig. 3), but only to the extent that differences among the fuel types actually existed. In addition, convective or radiative heating from the surrounding combustion environment (Morvan and Dupuy 2001), regardless of type, may have contributed to the discrepancy among fire behaviour distributions within fuel types. Fine scale differences in fuel loadings associated with each fuel type may also play a role in the variation in local heating. Typically higher fuel loads create conditions with more fuel compaction and physically interlaced fuel types. For example, plot two had higher average fuel loadings (0.579 *v.* 0.407 kg m^2) and range of loadings (0.416–1.009 kg m^{-2}) than plot one (0.303–0.617 kg m^{-2}).

Our results confirm that heterogeneity of fuel types, as detected by our fuel detection algorithm, and their biomass related well with spatial patterns of fire behaviour. Understanding pine litter accumulation may be of particular importance, given its high resin content and influence on fire behaviour (Fonda 2001; Hiers *et al.* 2009). Knowledge of the density, heights and distances to the nearby pine overstorey (O'Brien *et al.* 2008) could be coupled with models of forest matrix wind patterns (Smith *et al.* 1972) during seasons of needle-fall to project litter accumulation rates, distribution and loading across a larger fuelbed. Furthermore, tufts of grass suspend fallen pine litter, creating a well ventilated (Nelson and Hiers 2008) and interlaced fuelbed that determines the continuity of fire spread and adds to the heterogeneity of fire behaviour and fire effects, more so than with more homogeneous fuels (Hiers *et al.* 2009). The F layer may be affected by seasonal climate and decomposition patterns (Hendricks *et al.* 2002), but this fuel type was not determined to be a significant driver in the CART models. Furthermore, the F layer is often a small component of the fuelbed in frequently burned longleaf pine forests because there is little time for decomposition of leaf litter between burns. Applying the fuel proxy approach presented here, minimised the effects of loading by incorporating relative biomass approximations across fuel types. Quantifying the difference in loading between plots may improve future results. Predictions of fuel heterogeneity without fuel loading, however, are critical as measuring loading and fire behaviour within the same fuelbed remains problematic.

These results support previous research on fine-scale heterogeneity of fuel traits and fire behaviour found within this system (Hiers *et al.* 2009; Loudermilk *et al.* 2012) that may provide a link to understanding fire effects at the same scale (Mitchell *et al.* 2006; Thaxton and Platt 2006; Mitchell *et al.* 2009; Gagnon *et al.* 2012). Distinct to Loudermilk *et al.* (2012), this study used an advanced technique in classifying fuel types from high-resolution plot photography that provided thousands of sample points (image pixels). Loudermilk *et al.* (2012) was restricted to fuel type characterisation by field data collection (similar to this study's point-intercept approach) with under 170 sample points within the same area. Coupling sub-metre structural measurements of the fuelbed (see Loudermilk *et al.* 2012) and fuel type detection from both high-resolution imagery and field data may be promising for future work.

This variability at fine scales may have implications for understorey plant community mortality and assembly patterns in high species richness areas (Mitchell *et al.* 2009; Gagnon *et al.* 2012). If plant (or seed) mortality depends on exposure to combustion residence times (Wiggers *et al.* 2013), heterogeneity of fuel types may be an important factor. However, if plant mortality depends on total energy exposure, heterogeneity of fuel loadings should be considered (Gagnon *et al.* 2012). Exceptions may be found in particular fuel types, such as pine cones (Fonda and Varner 2004), which in our study burned longer (mean residence time = 187 s) and released greater radiant energy (mean FRE = 310 J) than any other fuel type (<70 s and <94 J).

Conclusions

We determined that the fuel recognition method in RR was sufficient for determining fuel types at a higher resolution than is possible with typical *in-situ* measurements, and these fine-scale fuels related well to fine-scale fire behaviour. Fuel types were comparable to field data, capturing dominant as well as less abundant, yet important fuel types. When linked with fire behaviour measurements at the same scale, fine-fuels (e.g. pine litter *v.* grasses) illustrated unique as well as coupled combustion properties. These fuel types, combined with other fuel attributes, determined non-linear fire behaviour characteristics. RR predicted fire spread well in a coarser scale grassland experiment (Achtemeier 2013), and using this model to simulate fire spread at the fine-scale is critical for understanding fire effects, such as understorey plant community assembly. Our next step in that process includes using the high-resolution distribution of fuels to model fire spread and fire spread rate using RR.

Acknowledgements

This study was funded through the National Fire Plan 01.SRS.A.5 and Joint Fire Science Program grant 09–1-01–7, and in part by the Strategic Environmental Research and Development Program of the Department of Defence, project RC-2243. This study was part of the Prescribed Fire Combustion and Atmospheric Dynamics Research Experiment (RxCadre), Joint Fire Science Program grant 11–2-1–11. We thank the Forestry Sciences Laboratory, Southern Research Station, USDA Forest Service, Athens, GA, USA, for their support.

References

Achtemeier GL (2013) Field validation of a free-agent cellular automata model of fire spread with fire–atmosphere coupling. *International Journal of Wildland Fire* **22**, 148–156. [Published online 25 September 2012] doi:10.1071/WF11055

Arroyo LA, Pascual C, Manzanera JA (2008) Fire models and methods to map fuel types: the role of remote sensing. *Forest Ecology and Management* **256**, 1239–1252. doi:10.1016/J.FORECO.2008.06.048

Berjak SG, Hearne JW (2002) An improved cellular automaton model for simulating fire in a spatially heterogeneous Savanna system. *Ecological Modelling* **148**, 133–151. doi:10.1016/S0304-3800(01)00423-9

Breiman L, Friedman JH, Olshen RA, Stone CJ (1984) 'Classification and Regression Trees.' (Eds PJ Bickel, WS Cleveland, RM Dudley) (Wadsworth, Inc.: Belmont, CA)

De'ath G, Fabricius KE (2000) Classification and regression trees: a powerful yet simple technique for ecological data analysis. *Ecology* **81**, 3178–3192. doi:10.1890/0012-9658(2000)081[3178:CARTAP]2.0.CO;2

Fonda RW (2001) Burning characteristics of needles from eight pine species. *Forest Science* **47**, 390–396.

Fonda R, Varner J (2004) Burning characteristics of cones from eight pine species. *Northwest Science* **78**, 322–333.

Gagnon PR, Harms KE, Platt WJ, Passmore HA, Myers JA (2012) Small-scale variation in fuel loads differentially affects two co-dominant bunchgrasses in a species-rich pine savanna. *PLoS ONE* **7**, e29674. doi:10.1371/JOURNAL.PONE.0029674

Grunwald S, Daroub SH, Lang TA, Diaz OA (2009) Tree-based modeling of complex interactions of phosphorus loadings and environmental factors. *The Science of the Total Environment* **407**, 3772–3783. doi:10.1016/J.SCITOTENV.2009.02.030

Hendricks JJ, Wilson CA, Boring LR (2002) Foliar litter position and decomposition in a fire-maintained longleaf pine–wiregrass ecosystem. *Canadian Journal of Forest Research* **32**, 928–941. doi:10.1139/X02-020

Hiers JK, O'Brien JJ, Mitchell RJ, Grego JM, Loudermilk EL (2009) The wildland fuel cell concept: an approach to characterize fine-scale variation in fuels and fire in frequently burned longleaf pine forests. *International Journal of Wildland Fire* **18**, 315–325. doi:10.1071/WF08084

Holliday P (2001) Going, going… saving the longleaf pine ecosystem before it's gone. In 'The Fire Forest: Longleaf Pine–Wiregrass Ecosystem', The Natural Georgia Series. pp. 55–68. (Georgia Wildlife: Atlanta, GA)

Keane RE, Burgan R, van Wagtendonk J (2001) Mapping wildland fuels for fire management across multiple scales: integrating remote sensing, GIS, and biophysical modeling. *International Journal of Wildland Fire* **10**, 301–319. doi:10.1071/WF01028

Kirkman LK, Mitchell RJ, Helton RC, Drew MB (2001) Productivity and species richness across an environmental gradient in a fire-dependent ecosystem. *American Journal of Botany* **88**, 2119–2128. doi:10.2307/3558437

Loudermilk EL, O'Brien JJ, Mitchell RJ, Cropper WP, Hiers JK, Grunwald S, Grego J, Fernandez-Diaz JC (2012) Linking complex forest fuel structure and fire behaviour at fine scales. *International Journal of Wildland Fire* **21**, 882–893. doi:10.1071/WF10116

Mitchell RJ, Hiers JK, O'Brien JJ, Jack SB, Engstrom RT (2006) Silviculture that sustains: the nexus between silviculture, frequent prescribed fire, and conservation of biodiversity in longleaf pine forests of the southeastern United States. *Canadian Journal of Forest Research* **36**, 2724–2736. doi:10.1139/X06-100

Mitchell RJ, Hiers JK, O'Brien J, Starr G (2009) Ecological forestry in the Southeast: understanding the ecology of fuels. *Journal of Forestry* **107**, 391–397.

Morvan D, Dupuy JL (2001) Modeling of fire spread through a forest fuel bed using a multiphase formulation. *Combustion and Flame* **127**, 1981–1994. doi:10.1016/S0010-2180(01)00302-9

Mutlu M, Popescu SC, Stripling C, Spencer T (2008) Mapping surface fuel models using LIDAR and multispectral data fusion for fire behavior. *Remote Sensing of Environment* **112**, 274–285. doi:10.1016/J.RSE.2007.05.005

Myers RL (1990) Scrub and High Pine. In 'Ecosystems of Florida.' (Eds RL Myers, JJ Ewel.) pp. 150–193. (University of Central Florida Press: Orlando, FL)

Nelson RM, Hiers JK (2008) The influence of fuelbed properties on moisture drying rates and timelags of longleaf pine litter. *Canadian Journal of Forest Research* **38**, 2394–2404. doi:10.1139/X08-078

O'Brien JJ, Hiers JK, Callaham MA, Mitchell RJ, Jack SB (2008) Interactions among overstory structure, seedling life-history traits, and fire in frequently burned neotropical pine forests. *Ambio* **37**, 542–547. doi:10.1579/0044-7447-37.7.542

Overing JD, Weeks HH, Wilson JP, Sullivan J, Ford RD (1995) Soil Survey of Okaloosa County, Florida. USDA Natural Resource Conservation Service, (Washington, DC)

Prasad A, Iverson L, Liaw A (2006) Newer classification and regression tree techniques: bagging and random forests for ecological prediction. *Ecosystems* **9**, 181–199. doi:10.1007/S10021-005-0054-1

R Core Team (2013) 'R: A Language and Environment for Statistical Computing.' (R Foundation for Statistical Computing: Vienna, Austria)

Smith FB, Carson DJ, Oliver HR (1972) Mean wind-direction shear through a forest canopy. *Boundary-Layer Meteorology* **3**, 178–190. doi:10.1007/BF02033917

Thaxton JM, Platt WJ (2006) Small-scale fuel variation alters fire intensity and shrub abundance in a pine savanna. *Ecology* **87**, 1331–1337. doi:10.1890/0012-9658(2006)87[1331:SFVAFI]2.0.CO;2

Varner JM, III, Kush JS, Meldahl RS (2000) Ecological restoration of an old-growth longleaf pine stand utilizing prescribed fire. In 'Fire and Forest Ecology: Innovative Silviculture and Vegetation Management. Tall Timbers Fire Ecology Conference Proceedings', 14–16 April 1998, Tallahassee, FL. (Eds WK Moser, CE Moser) pp. 216–219. (Allen Press, Inc.: Lawrence, KS, USA)

Wiggers MS, Kirkman LK, Boyd RS, Hiers JK (2013) Fine-scale variation in surface fire environment and legume germination in the longleaf pine ecosystem. *Forest Ecology and Management* **310**, 54–63. doi:10.1016/J.FORECO.2013.07.030

Appendix

Fig. A1. A FLIR SC660 thermal imaging system mounted on a 7 m-high tripod over an experimental fuel bed. Time-elapsed imagery is captured as a low-intensity fire spreads through the understorey (surface) fuelbed.

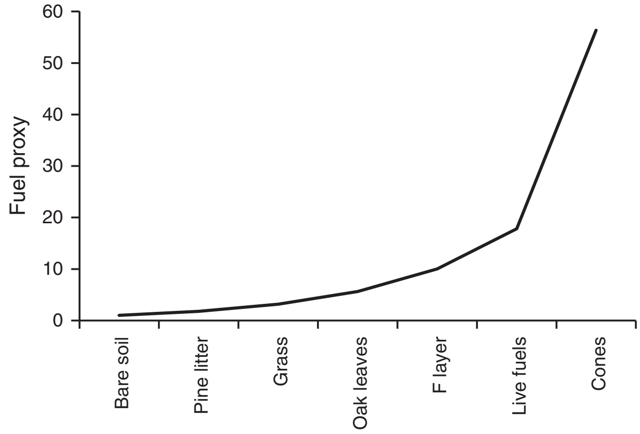

Fig. A3. Fuel proxy used to create a 'fuels' independent variable (for CART analysis) that incorporates influence from biomass and surface area of various fuel types developed from the fuel recognition method. Prior to conversion, fuel types were ordered according to approximate relative biomass to create fuel type categories (i.e. 0,1,2,3,4,5,7). The exponential function was fit to these category values, with longleaf pine cone biomass as a target upper limit (56.1 g, Fonda and Varner 2004). Fuel Proxy value = $\exp^{(\text{fuel type category} \times 0.576)}$, e.g. fuel proxy for pine cones = $\exp^{(7\times0.576)}$.

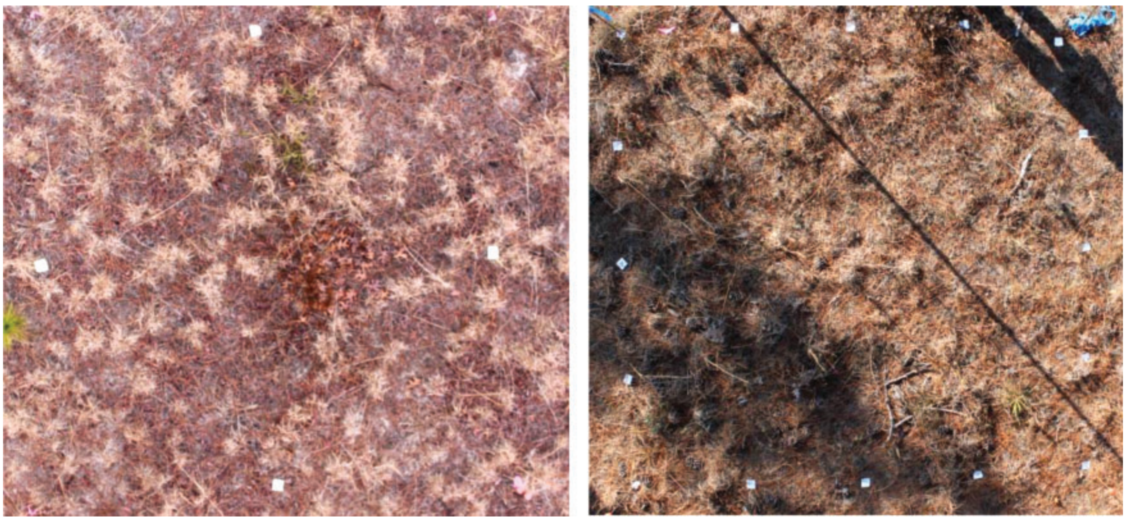

Fig. A2. Original high-resolution digital images of the fuelbed taken for plot 1 (left) and plot 2 (right). Images were cropped to 4×4-m area (aluminium markings) and oriented before image analysis.

Table A1. Residence times for temperatures exceeding 525°C for all fuel types

We calculated the combustion residence times within five 'cutoff' times or percentiles past which only a fraction of combustion at temperatures exceeding 525°C remains active. The value 525°C is considered the lower threshold for flaming combustion. These cutoff times are set at 50, 20, 5 and 1% of the initial combustion to correspond with residence time in the fuels matrix in Rabbit Rules (Achtemeier 2013). Results for grass and pine needles are common for the two burns. Fuel loadings for plot 1 were 23% higher than fuel loadings for plot 2, and residence times were more than twice as long in plot 2, mainly because of the presence of pine cones. Plot 1: With the exception of live fuels, there were sharp declines in residence times for all fuels from 100% to near 50% during the first 4 s of fire. Pine needles and the F layer showed the fastest decline in percentage and therefore the shortest residence times. The shorter residence times found for grass at 300°C (Fig. 3) were not found at 525°C. Longer residence times were found for live fuels. Analysis for total energy (not shown) found that in the range 5–50 J, variation among the dead fuels was less than 1%. Plot 2: With the exception of pine cones, there were similar declines in residence times for grass and pine needles from 100% to near 50% during the first 8 s of fire. The shorter residence times found for grass at 300°C (Fig. 4) were not found at 525°C. Longer residence times were found for pine cones. Residence times for temperatures exceeding 525°C for all fuel types during burns on 6 February 2011 (plot 1) and 11 February 2011 (plot 2)

Plot 1	Grass	Pine	F Layer	Live	Oak
50%	5.0	3.5	3.4	9.5	4.6
20%	12.2	10.8	9.0	17.5	12.4
5%	18.0	16.8	16.0	24.0	23.0
1%	23.0	23.0	23.0	27.5	32.0
Plot 2	**Grass**	**Pine**	**Cones**	**Live**	
50%	9.5	9.6	49.0	9.0	
20%	19.3	19.3	86.0	18.0	
5%	35.0	35.0	126.0	34.0	
1%	68.0	68.0	165.0	67.0	

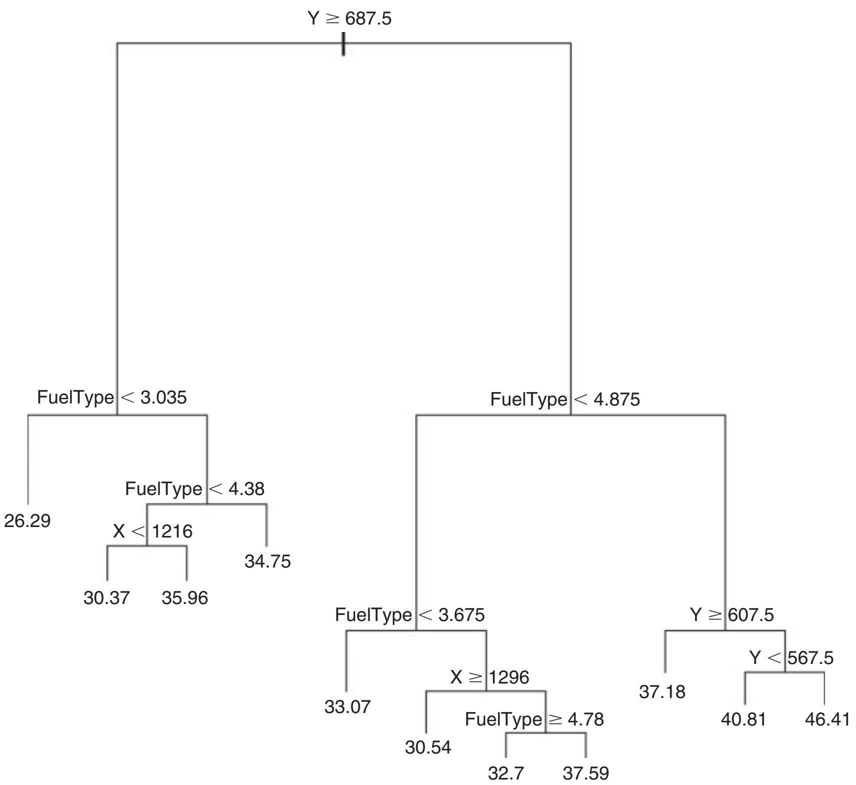

Fig. A4. Plot 1 CART tree output for model: Residence time (s) ~Fuels (fuel proxy), *x*-coordinate, *y*-coordinate, at the 33 × 33-cm scale. This illustrates several tree 'splits' or sources of explained variation, associated with pine litter *v.* grasses, as well as pine litter combined with grasses *v.* oak leaves combined with live fuels. See Fig. A2 for fuel proxy values. FuelType, fuel proxy.

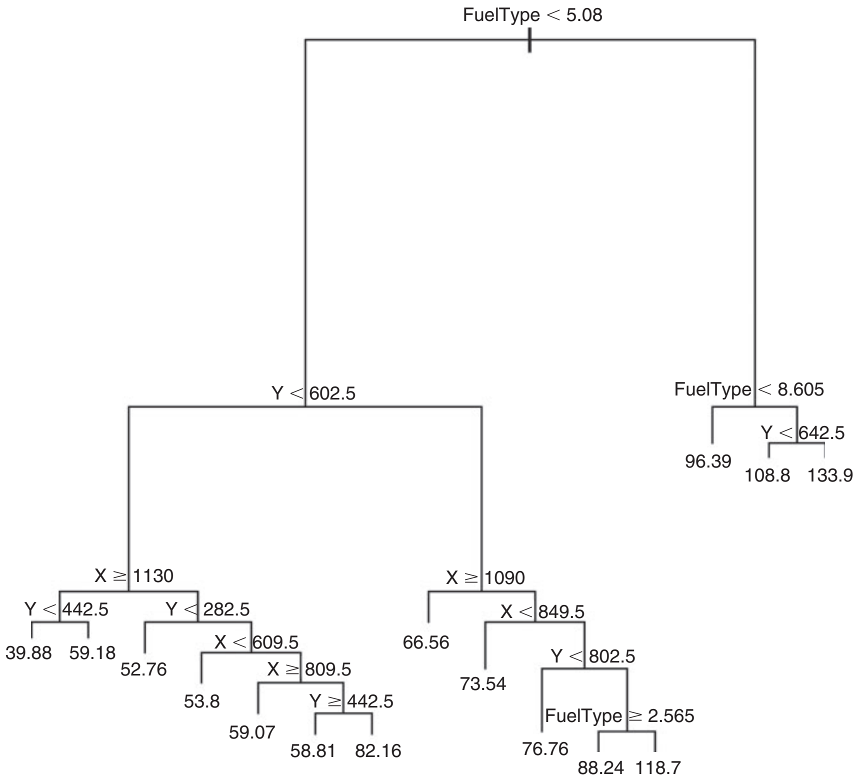

Fig. A5. Plot 2 CART tree output for model: Residence time (s) ~Fuels (fuel proxy), *x*-coordinate, *y*-coordinate, at the 33×33-cm scale. This illustrates several tree 'splits' or sources of explained variation, associated with pine litter *v.* grasses, as well as pine litter combined with grasses *v.* oak leaves combined with live fuels. See Fig. A2 for fuel proxy values. FuelType, fuel proxy.